110 KSME Journal, Vol.2, No.2, pp. 110~115, 1988.

EFFECT OF SINGLE OVERLOAD ON FATIGUE BEHAVIOR IN THE WELDED HAZ OF LOW ALLOY STEEL

Jae-Kyoo Lim*

(*Received October 4, 1988*)

Room temperautre fatigue crack growth behavior was obtained for 4140 parent steel, parent heat treated(same as PWHT), as-welded HAZ and PWHT HAZ material under $R \approx O$ constant amplitude loading and single tensile overloads with an over load ratio(OLR : P_{over}/P_{max}) of 2.5. Double pass automatic submerged arc welding with AWS EM2 electrode was used. PWHT was performed at 650℃ for one hour. Constant amplitude fatigue crack growth behavior was very similar for all four material conditions in the log-log linear Paris region. All material conditions responded favorably to the single tensile overloads with fatigue crack growth retardation ranging from 2.5×10^5 to 4.5×10^5 cycles which corresponded to life increases of 250 to 400 percent. SEM analysis indicated many similarities on the fatigue fracture surfaces with predominant ductile quasi-striation morphology.

Key Words : Welding HAZ, Fatigue Crack Growth, Single Overloads, Residual Stress, Crack Closure, Crack Retardation, Fractography, PWHT, Low Alloy Steel

1. INTRODUCTION

Design and research against unstable brittle fracture of welded structures and components is an active international problem(McHenry & Potter, 1988). Brittle fracture of welded structures often starts from the heat affected zone(HAZ) (Dolby, 1972 ; Burdekin, 1967). A weldment, especially the HAZ, is a very complicated and variable structure formed from different thermal and environmental conditions(Phillip, 1983 ; Frost et. al.,1981). These complexities involve inherent mechanical behavior such as strength, ductility, hardness and fracture toughness. In addition, three dimensional residual stress/strain can result in significant decrease of fracture toughness in the HAZ(Kameda et al., 1976 ; Dawes, 1976). Therefore, in welding low alloy steels such as 4140, post weld heat treatment(PWHT) is a common practice for removing undesirable residual tensile stresses along with welding and reheat for repairing(Suzuki et. al., 1976 ; Bloom, 1981). Very high PWHT, over 600℃, of these steels, however, can cause a coarse grained region near the fusion line of the HAZ resulting not only in embrittlement, but also in stress relief cracking(Hippsley et. al., 1980). Lim(Lim & Chung, 1988), using COD fracture toughness and fracture surface observations, showed that the degree of PWHT embrittlement is dependent upon heating rate, holding time, applied stress and grain size of the weld HAZ microstructure.

Most welded structures and components are subjected to variable amplitude loading. Initial cracks can then grow under cyclic load to fracture. Both high and low amplitude cycles along with constant amplitude cycles can occur in welded structures and components. Hence sequence, or interaction effects, are of importance in calculating fatigue crack growth life of weldments. High tensile overloads followed by low amplitude loading can involve appreciable retardation of fatigue creack growth. This retardation has been attributed to crack tip blunting, residual compressive stresses in front of the crack tip and to crack closure(ASTM STP 596, 1976). In order to better calculate fatigue crack growth life in weldments, this retardation influence must be known quantitatively. Very little fatigue crack growth retardation information exists for weldments.

Therefore, the purpose of this research is partially to contribute to the needed information for safe design and service life of weldments, particularly the HAZ and PWHT HAZ, subjected to both constant amplitude and single tensile overloads. This contribution is achieved using 4140 steel evaluated by fatigue testing and scanning electron microscopy(SEM).

2. TEST MATERIALS AND EXPERIMENTAL PROCEDURE

The parent material used in this research was 4140 vacuum degassed steel. Chemical composition and monotonic tensile properties in the rolled direction are given in Table 1 and 2 respectively. Steel plate with 25mm thickness was cut to 152×610mm sections and a U shaped groove, 610mm long, was cut perpendicular to the rolled direction. The U groove was then welded using an automatic submerged arc welder with two passes. The electrode used was AWS EN2 and the flux was AWS F9A6. The welding conditions are given in Table 3. Figure 1 shows the weld section configuration along with the position of compact type(CT) specimens used for all fatigue tests. A typical macroetched weld bead cross section is shown in Fig.2. The deposit metal appears as typical dendrite structure and the weld HAZ is located vertically for satisfactory extraction of CT specimens. Chemical composition of the electrode and deposit metal are given in Table 1

*Mechanical Design Department, Chonbuk National University, Chonju 560-756, Korea

Table 1 Chemical composition, % weight

	C	Mn	P	S	Si	Ni	Cr	Mo	Ti	V	Cu
4140 steel	0.39	0.81	0.005	0.016	0.11	0.11	0.90	0.17	—	0.04	—
Electrode	0.67	1.57	0.008	0.006	0.38	1.65	0.02	0.35	<0.01	<0.01	0.096
Deposit	0.07	1.38	0.013	0.006	0.31	1.42	0.09	0.30	<0.01	<0.01	0.11

Table 2 Monotonic tensile properties

Property	4140 steel	Weld deposit
Ultimate Strength, S_u-MPa	577	772
0.2% Yield Strength, S_y-MPa	338	598
True Fracture Stress, σ_f-MPa	1049	1177
True Fracture Strain, ε_f	0.33	0.24
Reduction in Area-%	54	42

Table 3 Welding conditions for submerged arc welding

Heat Input	30KJ/cm
Preheating temperature	200℃
Current	500A
Voltage	30V
Welding speed	30cm/min
Wire diameter	2.4mm

and monotonic tensile properties in the long direction of the weld deposit, obtained from tensile specimens, are given in Table 2.

The chevron notched specimens with $H/W=0.6$ were machined so that the fatigue crack would grow through the weld HAZ fusion line parallel to the weld direction and perpendicular to the rolled direction. Specifically, single tensile overload influence on constant amplitude loading was obtained under four material conditions as follows; parent material, heat treated parent material, as-welded HAZ material and PWHT HAZ material. Heat treatment was performed on both welded and parent material CT specimens as follows; heating rate=220℃/hr, heating temperature=650℃, hold time=1hr, cooling rate=110℃/hr.

All fatigue tests were performed at room temperautre using a closed-loop electrohydraulic test system in load control. One side of each specimen was polished in the crack growth region with progressively finer emery paper to 600 girt. Cracks were monitored on this polished surface using a 33x traveling microscope with stroboscopic illumination. Cracks were also occasionally monitored on the back side of the specimen to determine possible crack tip eccentricity during testing.

Constant amplitude reference tests were obtained with load ratio, $R=P_{min}/P_{max}$, of approximately zero using a positive haversine wave with a frequency of 15 to 25Hz. The constant amplitude data ranged from 10^{-8} to 10^{-6}m/cycle and, hence were in region II or the Paris log-log linear region. Single tensile overloads were applied at a crack length of 25mm with an overload ratio of 2.5 as shown in Fig. 3. Overloads were applied with a ramp wave at 0.125Hz. All tests, were terminated when the crack growth rate became too great to accurately meausre crack length or when the uncracked ligament of the specimen (w-a) ceased to be predominately elastic. Both these criteria were essentially at about fracture.

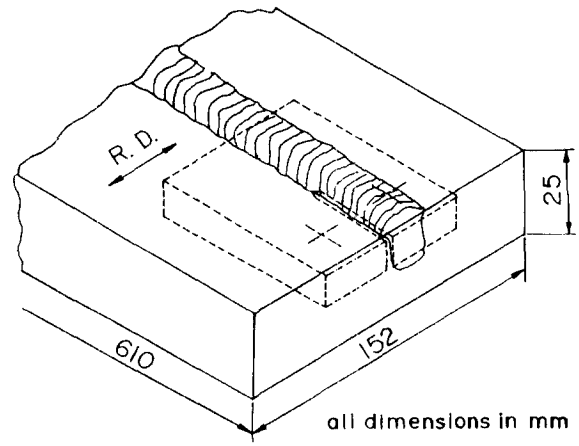

Fig. 1 Weld plate configuration and position of CT specimens

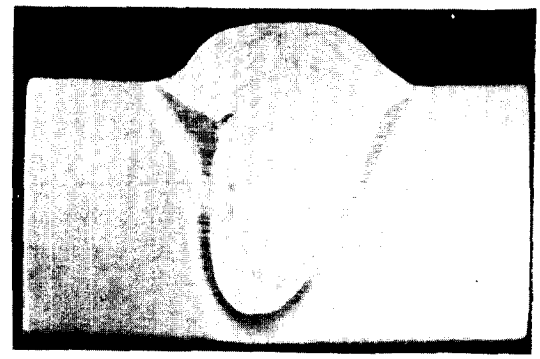

Fig. 2 Macroetch photograph of bead and plate weldment

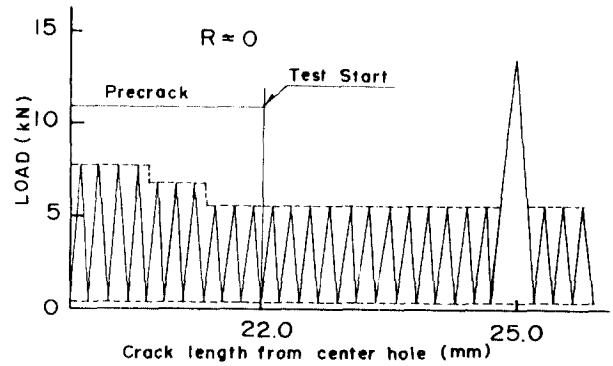

Fig. 3 Load spectrum for precracking, constant amplitude and tensile overload

All fatigue specimens were precracked approximately 2mm to a total crack length, a, of 22mm. Precracking was usually done in three load shedding steps as shown in Fig.3. The reduction of P_{max} between load steps was less than 20% according to ASTM standard E647(ASTM Standard E647, 1987). The maximum stress intensity factor, K_{max}, just prior to overload was 23.5 MPa $\sqrt{m}$ and the overload stress intensity factor, K_{OL}, was 59 MPa $\sqrt{m}$.

Crack length, a, versus applied cycles, N, data were reduced to da/dN versus $\triangle K$ using a second order incremental polynomial method for constant amplitude tests and a secant method for single overload tests.

3. TEST RESULTS AND DISCUSSION

3.1 Fatigue Crack Growth Behavior

The constant amplitude and single tensile overload crack length, a, versus applied cycles, N, curves are given in Fig.4 for all $R \approx 0$ tests. Since each constant amplitude test started at a=22mm and each single tensile overload test had the same overload applied at a=25mm, followed by the same P_{max} value, this figure provides substantial comparative results without reverting to da/dN versus $\triangle K$ curves. In Fig. 4, the constant amplitude data are represented by open data points and labeled no overload, and the overload data are represented by solid data points or crosses within the symbol. Also for a given material condition, data points with the same shape are used for the constant amplitude test and for the overload test. These selections make for easier comparison. The general schematic a versus N curve for the no overload curve and the overload curve is shown in Fig.5. The retardation cycles, N_R, is defined in Fig.5. N_R is the horizontal displacement of the a versus N curve following a single tensile overload.

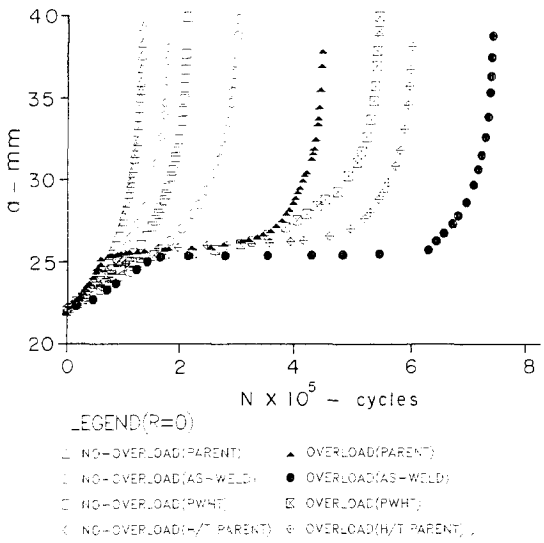

Fig. 4 Crack growth for no overload and single overload conditions

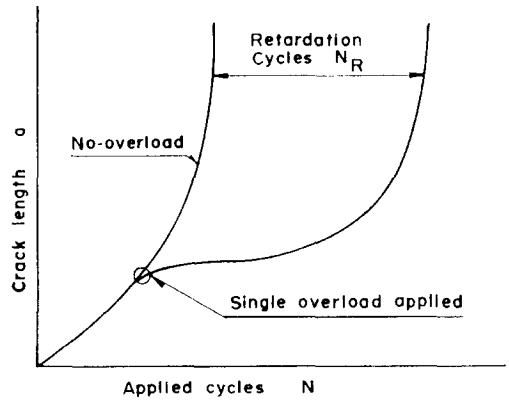

Fig. 5 Schematic diagram of fatigue crack growth retardation

From Fig.4, the constant amplitude fatigue crack growth curves were smooth and continuous and varied by a factor of only two or less at fracture for the given material conditions. This is a very small variation. Fatigue life is increasing the order as follows, parent, heat treated parent, PWHT and as-weld at the no overload, that is, fatigue life of parent is increasing after heat treatment, but that of the welded HAZ is opposite. At single overload, all materials are retardation of crack propagation. Retardation of as-weld is the greatest. Da/dN versus $\triangle K$ curves for all constnat amplitude tests using the incremental second order polynomial method are shown on upper side of Fig.6. The data are essentially log-log linear and hence satisfy the region II Paris equation.

From Fig.4, the overload cycles to failure for a given R ratio fell within a factor of about 2.5 or less for all material test conditions, This again is a rather small variation between materials. The number of cycles of retardation, N_R, varies from about 2.5×10^5 to 4.5×10^5cycles. This represents fatigue crack growth life increases from about 250 to 450% for $R \approx O$. This indicates that all the material conditions investigated responded favorably to the single tensile overloads. The as-welded HAZ material with its higher strength had the greatest response to the single overloads compared to the other lower strength materials. This difference in retardation with strength agrees with results by others(Njus & Stephens, 1977; Petrak & Gallagher, 1975). However, the differneces in fatigue crack growth for the as-welded HAZ versus the other materials must also incorporate residual stresses that have not been relaxed through PWHT. In fact, as-welded HAZ material and PWHT HAZ material have the same microstructure, but differ essentially

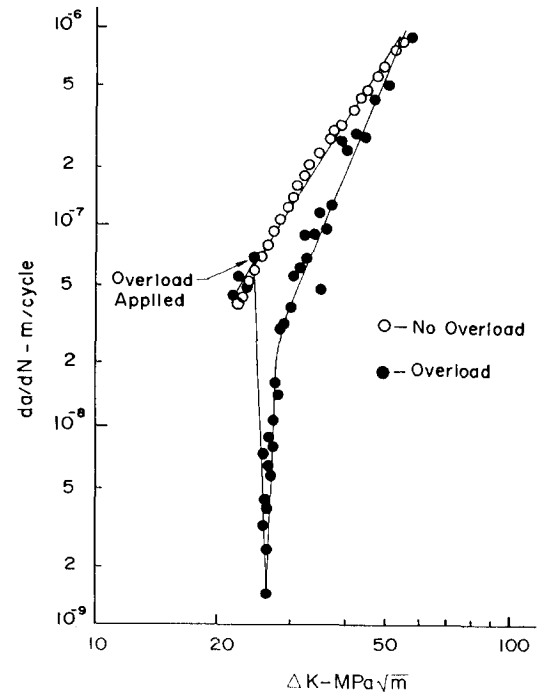

Fig. 6 Fatigue crack growth rate versus $\triangle K$ for no overloas and single overload, parent metal

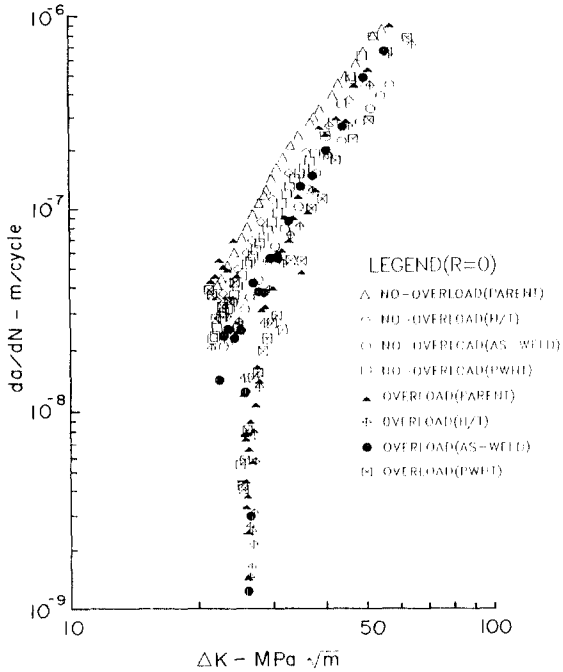

Fig. 7 Fatigue crack growth rate versus △K, all materials

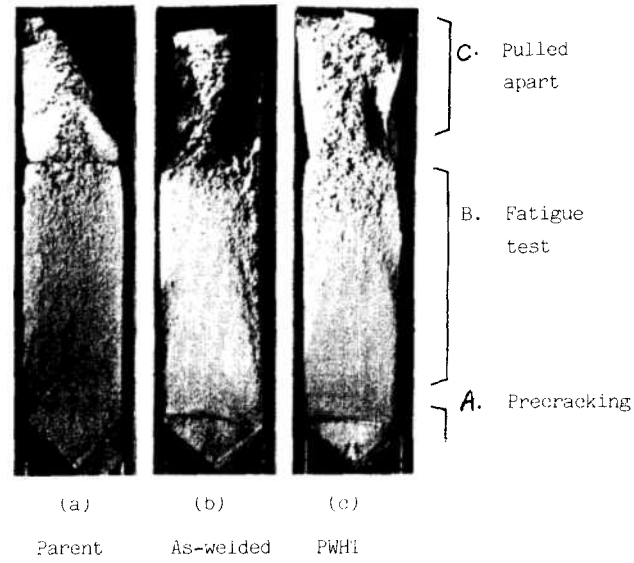

Fig. 8 Typical macro fracture sufaces for constant amplitude tests

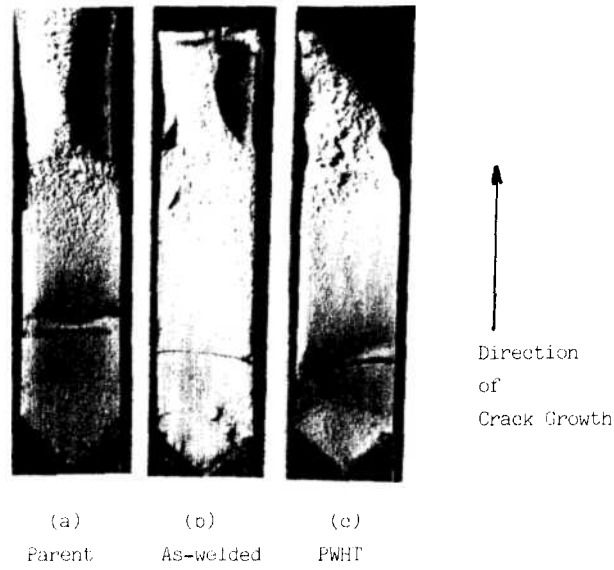

Fig. 9 Typical macro fracture surfaces for single overload tests

in residual stress. Thus both strength and residual stresses are involved with the fatigue crack growth retardation.

The a versus N data for all tests were reduced to da/dN versus $\triangle K$. Typical results for the no overload and overload conditions are shown in Fig.6 for the parent metal. Crack growth rates prior to the single tensile overload were above 10^{-8}m/cycle while after the single overload the rate dropped to almost 10^{-9}m/cycle. Converging of the no overload and overload data occurs as the crack grows out of the effective oveload region. A superposition of no over load and overload data similar to Fig.6 is shown in Fig.7 for all materials. Open data points represent no overload behavior. Greater scatter exists for the $R \approx O$ tests, however all material tests again exhibit similar behavior. Since crack closure was not monitored in these tests, an effective $\triangle K$ analysis cannot be made.

3.2 Macrofractography

Typical macro fracture sufaces are shown in Fig. 8 for the constant amplitude test and in Fig. 9 for the single overload tests. Three regions labeled A-C are shown in Fig.9. Label A indicates the precrack region and boundary, Label B denotes the fatigue crack growth test region and label C represents the final ductile fracture region. In all cases, the fatigue cracks initiated at the chevron and grew toward the top of the fractograplhs. In all cases, the constant amplitude fatigue crack growth regions are rather smooth. The single overload fracture sufaces indicate the overload marks are more intense. The overload crack tip curvature is somewhat eccentric, however, the curvature still satisfied ASTM E 647 requirements. The overloads markings indicate a small difference in the 25mm crack length at overload existed. This was not a significant factor however.

3.3 Scanning Electron Microscopy (SEM)

Typical SEM fractographs for the constant amplitude tests with the parent, as-welded HAZ and PWHT conditions are shown in Fig.10. Two magnifications are shown for each material condition. The direction of fatigue crack growth is from bottom to top in all fractographs. Very few distinct striations were evident on any of the surfaces, however so-called ductile quasi-striation crack grwoth morphology existed. All materials showed porosity, inclusions and secondary cracking, and appeared rather similar except the as-welded and PWHT material had more debris, more microcracks and greater roughness.

Fig.11 shows the effect of the single tensile overload for the parent, as-welded HAZ and PWHT material conditions. Again two magnifications are used for each material condition. The upper fractographs, taken at 100× or 200× magnification, show the tensile overload markings. The lower fractographs show the fracture surface at 100× magnification after the overload was applied. Substantial crack closure following the overload often tended to obscure some

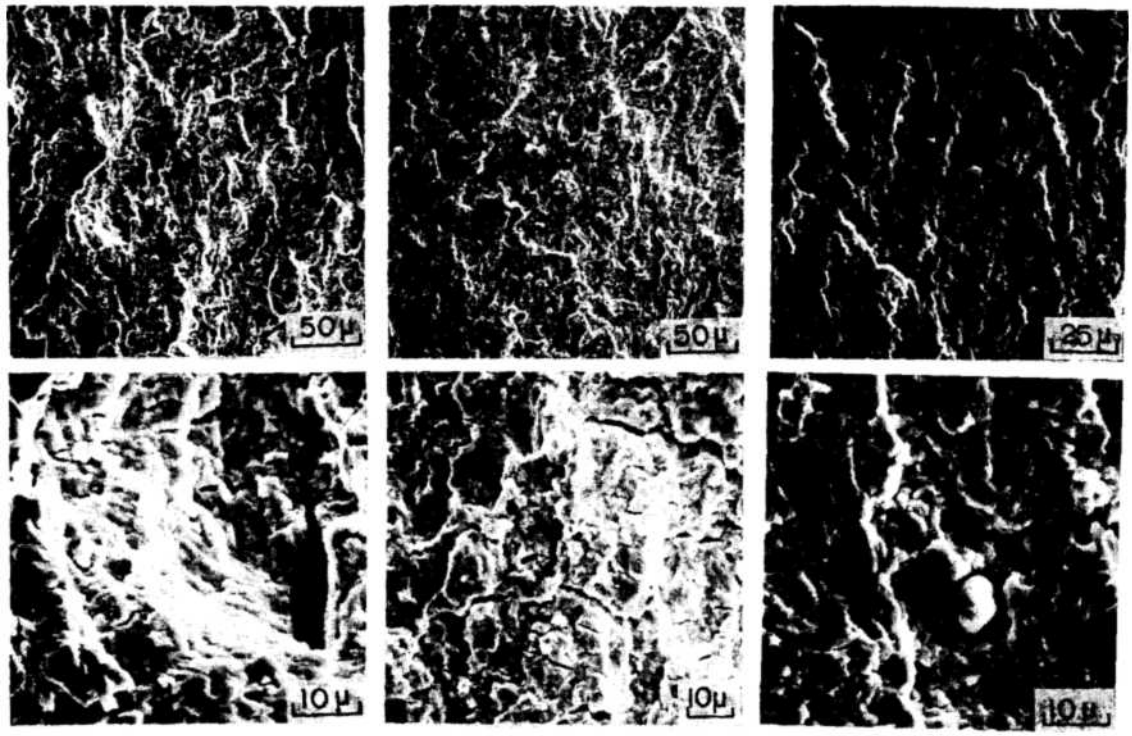

(a) Parent metal (b) As-welded HAZ (c) PWHT HAZ

Fig. 10 Typical SEM fractographs, no overload

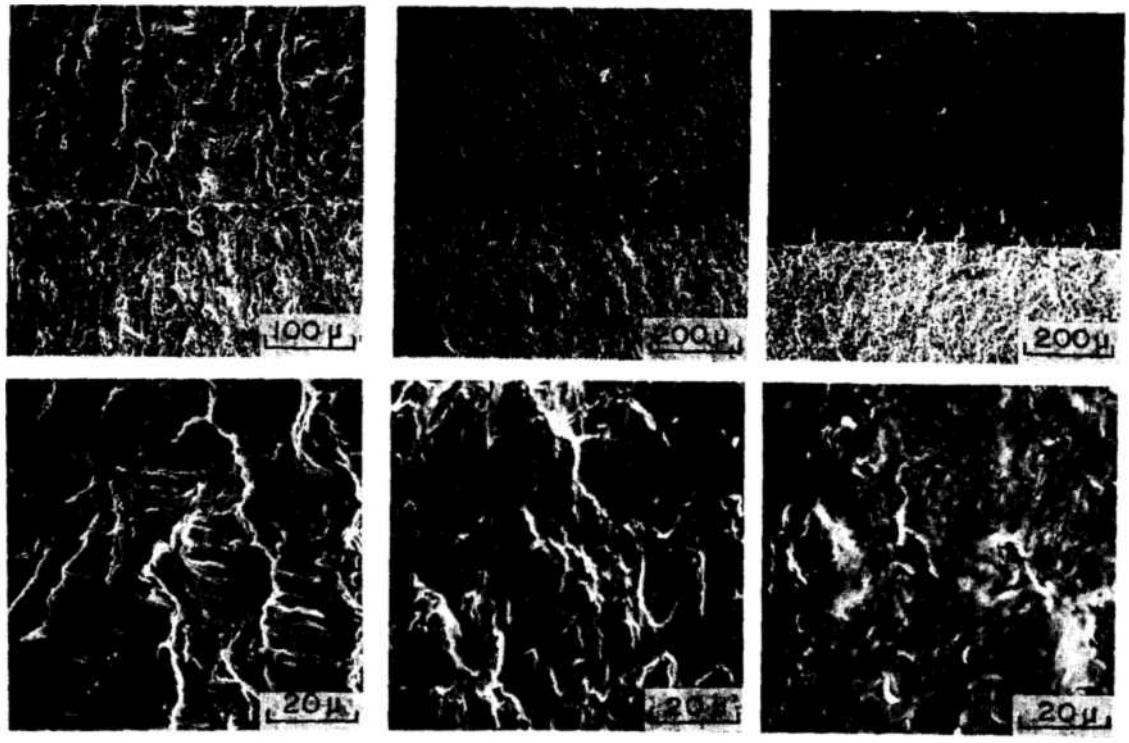

(a) Parent metal (b) As-welded HAZ (c) PWHT HAZ.

Fig. 11 Typical SEM fractographs, after single overload

of the fatigue crack growth markings. In general, no great differences in the fatigue crack growth morphology existed between the different material conditions tested. This is consistent with the lack of substantial differences between material conditions.

4. SUMMARY AND CONCLUSIONS

The following information is based upon room temperature fatigue crack growth and SEM investigations of the 4140 parent material, parent heat treated material(same as PWHT), as-welded HAZ material using automatic submerged arc welding and PWHT HAZ material subjected to constant amplitude loading(no-overload) and single tensile overloads using an OLR of 2.5.

(1) All four material conditions had essentially the same constant amplitude fatigue crack growth resistance in the Paris log-log linear region. Differences in fatigue life and fatigue crack growth rates were within a factor or two.

(2) All four material conditions responded favorably to the single tensile overloads. The differences between material response for theses single overloads was small, within a factor of 2.5.

(3) Retardation of fatigue crack growth varied from 2.5×10^5 to 4.5×10^5 cycles for the four material conditions which represented an increase in fatigue crack growth life from 250 to 400 percent. The greatest retardation response occurred in the as-welded HAZ material.

(4) SEM results indicated many similarities in fatigue crack growth morphology for the four material system. Ductile quasi-striations, porosity, inclusions and secondary cracking were evident with all four material conditions. The principal differences were the greater amounts of debris, microcracks and roughness in the as-welded and PWHT HAZ materials.

REFERENCES

ASTM Standard E647, 1987, "Standard Test Method for Constant Load Amplitude Fatigue Crack Growth Rates Above 10m/cycle", 1987 Annual Book of ASTM Standards, Vol 03.01 pp. 711~731.

ASTM STP 596, 1976, Fatigue Crack Growth Under Spectrum Loads.

Bloom, J.M.,1981, "An Analytical Assessment of the Effect of Residual Stress and Fracture Properties on Service Performance of Various Weld Repair Processes", Journal of Pressure Vessel Technology, ASME, Vol. 103, pp.373~397.

Burdekin, F.M.,1967, "Initiation of Brittle Fracture in Structural Steels", British Welding Journal, Vol. 12, pp.649~657.

Dawes, M.G., 1976 "Weld Metal Fracture Toughness", Welding Journal, Dec, pp.1052~1059.

Dolby, R.E.,1972, "Welding and Fracture Initiation in OT Low Alloy Steels", Metallurgy, pp.159~165.

Frost, R.H. Edwards, G.R. and Rheinlander, A.D.,1981, "A Constitutive Equation for the Critical Energy Input during Electroslag Welding", Welding Journal, Jan. pp.1s~6s.

Hippsley, C.A. Knott J.F. and Edwards, B.C.,1980, "A Study of Stress Relief Cracking in 2-1/4 Cr-1Mo Steel", Acta Metallurgica, Vol. 28, pp.869~885.

Kameda, J. Takahashi, H. and Suzuki, M. 1976, "Residual Stress Relief and Local Embrittlement of Weld HAZ in Reaction Pressure Vessel Steel", IIW Doc. No. X-800-76 and Doc. No. IX-1002-76.

Lim, J.K. and Chung, S.H., 1988, "Stress Effect on PWHT Embrittlement", Fatigue and Fracture Testing of Weldmemts, Edited by H.I.McHenry and J.M. Potter, ASTM STP, to be published.

McHenry, H.I. and Potter, J.M., 1988, Editors, Fatigue and Fracture Testing of Weldments, ASTM STP to be published.

Njus, G.O. and Stephens, R.I.,1977, "The Influence of Yield Strength and Negative Stress Ratio on Fatigue Crack Growth Delay in 4140 Steel", International Journal of Fracture, Vol. 13, No.4, pp.455~466.

Petrak G.I. and Gallagher J.P., 1975, "Predictions of the Effect Yield Strength on Fatigue Crack Growth Retardation in HP-9Ni-Co-30 C Steel", Journal of Engineering Material and Technology, pp. 206~213.

Phillip, R.H., 1983, "In Situ Determination of Transformation Temperature in the Weld Heat Affected Zone", Welding Journal, Jan. pp.12s~18s.

Suzuki, M. Takahashi, H. and Kameda, J., 1976, "Post Weld Heat Treatment and Embrittlement of Weld HAZ in a Low Alloy Steel", Welding Journal of JWS, Vol. 45, No. 1, pp. 6~13.